A model for the action of external current onto excitable tissue.

V.N. Biktashev[1,2], A.V. Holden[2,*] and H. Zhang[2]

November 15, 1996

[1] Institute for Mathematical Problems in Biology, Pushchino, Moscow region, 142292, Russia
[2] Physiology Department and Centre for Nonlinear Studies, The University, Leeds, LS2 9JT, UK
[*] Author to whom the correspondence should be addressed

Abstract

We outline a mathematical model of the action of an external electric current on excitable tissue, which considers the action of the current on different parts of the cell membrane within an ODE description. This model is intuitively clear and numerically efficient, and is used to predict and compute the defibrillation threshold for cardiac tissue.

1 Introduction

Extracellular stimulation by large (0.1–10 KV) and brief (0.01–5 ms) pulses applied by remote electrodes is widely used in clinical and experimental physiology to excite activity in nervous and muscular tissue: an important area of application is in pacing the heart [Zipes & Jalife, 1995]. Such field stimulation is also used to defibrillate heart muscle *i.e.* to eliminate all propagating activity when abnormal, re-entrant propagation is generating a life-threatening arrhythmia [Panfilov & Holden, 1996].

For a single cell in such a field, the current that flows in must equal the current that flows out of the cell, and so any effect must be generated by nonlinear summation of different behaviours of different parts of the cell. There must be potential gradients across the cell, and so each cell needs to be considered as a spatially extended object [Plonsey & Barr, 1986] and modelled by a partial differential system, as in [Cartee & Plonsey, 1992].

Here we present a simple ODE approach to the effects of extracellular field stimulation on excitable cells and tissues and apply it to estimate the defibrillation threshold for a model of mammalian ventricular tissue. We apply the singular perturbation approach of Krassowska and Neu [1994] to high-order biophysical excitation equations [Boyett *et al.* , 1996] and extend the excitable medium models of cardiac tissue [Biktashev & Holden, 1996] to include the effects of external current inputs, and illustrate defibrillation *via* the theory of Pumir & Krinsky [1996]. Recent approaches to the theoretical basis of defibrillation [Keener, 1996, Pumir & Krinsky, 1996] lead to to coupled partial differential systems.

2 Basic Equations

Biophysical membrane excitation equations are of the form:

$$\begin{aligned} C\partial_t u &= f(u,v,w), \\ \partial_t v &= g(u,v,w), \\ \partial_t w &= h(u,v,w), \end{aligned} \tag{1}$$

where $u = u(t)$ is the transmembrane voltage, C is specific membrane capacitance, f is transmembrane current density, vector $v = v(t)$ describes the fast gating variables, and vector $w = w(t)$ comprises slow gating variables and intra- and extra-cellular ionic concentrations, and g and h describe their kinetics. The variables u and v have comparable characteristic times. There are a number of different membrane ionic current models, for the same, and different parts of the heart. These models, that define the functions f, g and h are reviewed in [Zipes & Jalife, 1995], [Gray & Jalife, 1996] and [Panfilov & Holden, 1996]. In the illustrations of this paper we have used the Noble *et al.* [1990] model for the guinea pig ventricular cell, incorporated in a tissue model in [Biktashev & Holden, 1996].

We begin with a bidomain approach, for a single isolated cell with an intracellular domain , $\mathcal{I}$, external domain, $\mathcal{E}$, and the membrane surface, $\mathcal{M}$, and introduce the electrostatic potential ϕ_i and ϕ_e in $\mathcal{I}$ and $\mathcal{E}$, u_i and u_e as limit values of ϕ_i and ϕ_e at $\mathcal{M}$, and electric charge densities q_i and q_e at the inside and outside surface of the membrane.

1) Intracellularly, electroneutrality of the cytoplasm means for $\mathbf{r} \in \mathcal{I}$,

$$\nabla(\sigma_i \nabla \phi_i) = 0, \tag{2}$$

for a scalar specific conductivity σ_i. Here and below, $\mathbf{r}$ denotes the vector of coordinates of a point in space.

2) In the extracellular domain, electroneutrality means for $\mathbf{r} \in \mathcal{E}$:

$$\nabla(\sigma_e \nabla \phi_e) = 0, \tag{3}$$

for a scalar specific conductivity σ_e, and for a homogeneous external field $\mathbf{E}$,

$$\phi_e \sim (\mathbf{E}, \mathbf{r}),\ \mathbf{r} \to \infty. \tag{4}$$

In the case of a tissue of cells, Eq. (4) is to be replaced - *e.g.* for cells in a regular 3-dimensional grid, the domain $\mathcal{E} \cup \mathcal{I} \cup \mathcal{M}$ forms the elementary volume of the grid, and (4) is to be replaced by periodic boundary conditions for the "own" cell potential

$$\phi_{own}(\mathbf{r}) = \phi_{i,e}(\mathbf{r}) - (\mathbf{E}, \mathbf{r}),$$

or the "oscillatory component" of the potential, in terminology of Plonsey & Barr [1986] and Krassowska *et al.* [1990].

3) In the membrane, the boundary conditions of the "volume equations" (2,3) for $\mathbf{r} \in \mathcal{M}$:

$$\phi_i = u_i, \tag{5}$$

$$\phi_e = u_e, \tag{6}$$

and surface balance of charges on the interior and exterior sides of the membrane;

$$\partial_t q_i = \Sigma_i \Delta_M u_i - f(u) + \sigma_i(\nabla \phi_i, \mathbf{n}), \tag{7}$$

$$\partial_t q_e = \Sigma_e \Delta_M u_e + f(u) - \sigma_e(\nabla \phi_e, \mathbf{n}), \tag{8}$$

here f, is the transmembrane current, $\Sigma_{i,e}$ are specific conductivities, and Δ_M is the Laplacian operator on the membrane surface. For simplicity of notations, we assume here that $\Sigma_{i,e}$ are constant. Electroneutrality of a membrane element gives

$$q = q_e = -q_i. \tag{9}$$

The membrane capacitance is

$$Cu = q \tag{10}$$

and transmembrane voltage is

$$u = u_e - u_i. \tag{11}$$

After defining $f(\mathbf{r}, t), \mathbf{r} \in \mathcal{M}$, through local values of u, v and w, and local kinetic equations for v and w from (1), these equation form a closed system, which determines evolution of the distribution of electric properties over the cell at given $\mathbf{E}(t)$, and so describe the action of the external electric field onto the cell.

3 Reduction to the Membrane

Following the ideas of Krassowska and Neu [1994] we will now simplify this extensive nonlinear system of partial differential equations; note that in the electric part of the equations, all the nonlinearity is located in the term $f()$, and the remaining linear problem can be (in principle) solved. Summing the Eqs. (7) and (8), we get a linear equation

$$\Sigma_i \Delta_M u_i + \Sigma_e \Delta_M u_e = (\sigma_e \nabla \phi_e - \sigma_i \nabla \phi_i, \mathbf{n}), \qquad \mathbf{r} \in \mathcal{M} \tag{12}$$

for the overall current balance of the membrane element, which, together with the equations

$$\begin{array}{ll} \nabla(\sigma_i \nabla \phi_i) = 0, & \mathbf{r} \in \mathcal{I}, \\ \phi_i = u_i, & \mathbf{r} \in \mathcal{M}, \\ \nabla(\sigma_e \nabla \phi_e) = 0, & \mathbf{r} \in \mathcal{E}, \\ \phi_e = u_e, & \mathbf{r} \in \mathcal{M}, \\ u_e - u_i = u, & \mathbf{r} \in \mathcal{M}, \\ \phi_e \sim (\mathbf{E}, \mathbf{r}), & \mathbf{r} \to \infty, \end{array} \tag{13}$$

constitute a well posed elliptic problem for finding $u_{i,e}$ and $\phi_{i,e}$ at given $\mathbf{E}$ and u. Differentiation of (10) by time and substituting into (7) or (8), together with the slow equations, yields then the resulting system of equations of the form

$$\begin{aligned} C\partial_t u &= f(u,v,w) + \hat{L}u + \hat{I}\mathbf{E}, \\ \partial_t v &= g(u,v,w), \\ \partial_t w &= h(u,v,w), \end{aligned} \tag{14}$$

where u, v and w are now functions of time and position on the membrane, $\hat{L}$ is a linear (generally, integro-differential) operator in a space of scalar functions on the membrane, and $\hat{I}$ is a linear operator mapping vectors $\mathbf{E}$ to scalar functions on the membrane. The specific forms of $\hat{L}$ and $\hat{I}$ depend on the geometry of $\mathcal{M}$ and on the coefficients $\sigma_{i,e}$ and $\Sigma_{i.e}$. We use the following properties of these operators:

- $\hat{L}u$ vanishes if u is spatially homogeneous over the membrane,
- the integral of $\hat{L}u$ over the membrane surface is zero for any u, and
- the integral of $\hat{I}\mathbf{E}$ over the membrane surface is zero for any $\mathbf{E}$.

These properties follow from the derivation of (14). $\hat{L}u$ represents the currents between different loci of membrane, both through interior and exterior domains, and $\hat{I}\mathbf{E}$ is the additional current due to the external field.

4 Simplified Two-Compartment Model

We now construct a simplified model, that retains the main features of (14). We approximate all functions $u(x)$, $v(x)$ and $w(x)$ by piecewise constant functions, taking, at each time instant only two values at two different and fixed parts of the membrane. Denoting the two parts of the membrane by indices + and −, system (14) is then rewritten in the form

$$\begin{aligned} C\partial_t u_+ &= f(u_+, v_+, w_+) + \alpha(u_- - u_+) + I_{ext}(t), \\ C\partial_t u_- &= f(u_-, v_-, w_+) + \alpha(u_+ - u_-) - I_{ext}(t), \\ \partial_t v_\pm &= g(u_\pm, v_\pm, w_\pm), \\ \partial_t w_\pm &= h(u_\pm, v_\pm, w_\pm), \end{aligned} \tag{15}$$

where the signs in the last two equations are either all + or −.

In writing this system, we have taken into account the main properties of $\hat{L}$ and $\hat{I}$ listed in the previous section. The constant α of the dimensionality of conductivity in (15) should be positive; it is the effective conductivity of the cell in this two-compartment approximation. $I_{ext}(t)$ is the current produced by the external source and crossing the cell.

5 Quasi-Stationary Approximation

The system (15) contains a singular small parameter, the ratio of the characteristic times of the intracellular conductivity α, τ_α, and of the membrane excitability, τ_f. Biophysical data [Weidmann, 1952] give the intracellular resistivity of the order of 250 Ohm·cm, which for the cell size of 10-80 μm gives α of the order of several μS, so $\tau_\alpha \sim 10-100\mu$s, which is much less than $\tau_f \sim 1\ ms$. Numerical calculations of the simplified two-compartment model (15) would require time steps not greater than τ_α, while if we can get rid of the small parameter, times steps of around τ_f would be adequate.

We exclude the small parameter α by "quasi-stationary" arguments. Rewrite the first two equations of (15) as

$$C\partial_t U = \frac{1}{2}(f(U+\delta, v_+, w_+) + f(U-\delta, v_-, w_-)) \tag{16}$$

$$C\partial_t \delta = \frac{1}{2}(f(U+\delta, v_+, w_+) - f(U-\delta, v_-, w_-)) - 2\alpha\delta + I_{ext}(t) \tag{17}$$

where

$$U = \frac{1}{2}(u_+ + u_-),$$

and

$$\delta = \frac{1}{2}(u_+ - u_-).$$

Now, in (17) the term $-2\alpha\delta$ dominates over $\frac{1}{2}(f()-f())$, and omitting the nonlinear term $\frac{1}{2}(f()-f())$, (17) becomes a linear equation. If the characteristic time of I_{ext} change is bigger than τ_α, then this equation describes the fast approach of δ to its quasi-stationary value,

$$\delta_\infty(t) = \frac{1}{2\alpha} I_{ext}(t),$$

and we can substitute this value into (16), which yields

$$C\partial_t U = \frac{1}{2}(f(U+\delta_\infty(t), v_+, w_+) + f(U-\delta_\infty(t), v_-, w_-)). \tag{18}$$

Equations (18) and the last pair of (15) form a closed system, which depends only on the ratio I_{ext}/α. If we assume that the duration of pulses I_{ext} is shorter than the characteristic time τ_h of the slow variables then $w_+ \approx w_- \approx W$. This final simplification gives:

$$\begin{aligned} C\partial_t U &= \frac{1}{2}(f(U+\frac{1}{2\alpha}I_{ext}(t), v_+, W) + f(U-\frac{1}{2\alpha}I_{ext}(t), v_-, W)), \\ \partial_t v_\pm &= g(U \pm \frac{1}{2\alpha}I_{ext}(t), v_\pm, W), \\ \partial_t W &= h(U, \frac{v_+ + v_-}{2}, W). \end{aligned} \tag{19}$$

This model is almost as simple as the original (1) ordinary differential equation (*e.g.* , it has three equations more than the 17 variable Noble *et al.* [1990] ordinary differential system we use for ventricular excitation), but describes the effect of external current. This has been obtained from (15) assuming the characteristic time of the external curent pulses, τ_I, is

$$0.1\ ms \sim \tau_\alpha \ll \tau_I \sim \tau_f \sim \tau_g \ll \tau_h \sim 10\ ms.$$

In practice τ_I, τ_f and τ_g are all of the order of 1 ms.

The general model (14) can be simplified by quasi-stationary arguments to

$$C\partial_t U = \int\limits_{\mathcal{M}} f(U + \hat{L}^{-1}\hat{I}\mathbf{E}\,(t)\,, v, W)\; d\mathcal{M}, \tag{20}$$

with separate ordinary differential equations for v at each point of the membrane. If the external field $\mathbf{E}$ is fixed in direction and varies only in magnitude, then the surface integral in (20) can be reduced, in a Lebesgue style, to an ordinary integral

$$C\partial_t U = \int f(U + sE\,(t)\,, v, W)\, K(s)\; ds, \tag{21}$$

where the kernel $K(s)$ is determined by the cell geometry, the conductivities, and the direction of the external field, and because of electroneutrality of the cell

$$\int K(s)\, ds = 1.$$

The simple model (19) corresponds to evaluation of the integral in (21) at two points $s = \pm\frac{1}{2\alpha}$.

Below we explore numerically some properties of the model (19) and its generalisation to spatially extended media. To validate the two-point approximation of the integral (21), we compare the two-point results with those of a five-point evaluation of (21), in the form

$$\begin{aligned} C\partial_t U &= \frac{1}{5}\sum_{j=-2}^{2} f(U + \frac{j}{3\alpha} I_{ext}(t), v_j\,, W), \\ \partial_t v_j &= g(U + \frac{j}{3\alpha} I_{ext}(t), v_j\,, W),\ j = -2, \ldots, 2 \\ \partial_t W &= h(U, \frac{1}{5}\sum_{j=-2}^{2} v_j\,, W). \end{aligned} \tag{22}$$

6 Action onto a Single Cell

First we verify the quasi-stationary exclusion of the small parameter in transforming from (15) to (19) by studying the excitation processes in these two systems, and accuracy of the two-point approximation in (21) by comparision with the results of the five-compartment model (22). The kinetics $f()$, $g()$ and $h()$ were described by guinea pig ventricle myocyte model of Noble *et al.* [1990], that has 17 kinetic variables. α was 10μ S, which is consistent with data of Plonsey & and Barr [1986]. In the vector v we included the three fastest gating variables 'h', 'd' and 'f'; gate 'm' was not a dynamic variable but a fixed function of u. Thus, model (19) contained 20 ODEs, as opposed to 34 ODEs and large values of the parameters α and I_{ext} in (15), and 29 ODEs in the five-compartment version (22).

We obtained the strength-duration curve — the threshold external current I_{ext} as a function of stimulus duration (Fig. 1). The results obtained for the three models (15), (19) and (22) coincide with a good precision. Thus α is large enough for the quasi-stationary approximation to be valid, and two-point evaluation of the surface integral gives reasonable accuracy, and in all other numerical experiments we used only model (19).

The threshold current was also determined at a stimulus duration of 2 ms and different intervals after a preceding action potential. The excitability of the biophysical excitation equations for cardiac tissue is highly dependent on the history of the cell activity. Intervals between action potentials as short as those in Fig. 2 cannot be achieved by a pair of stimuli applied to a resting cell, as they are less than the standard (from rest) action potential duration. Since we are specially interested in the defibrillation threshold, the cell has been preconditioned by an excitation sequence identical to that of a point in a developing spiral wave during first 14 rotations; in this model, the average period of the spiral wave is around 102 ms.

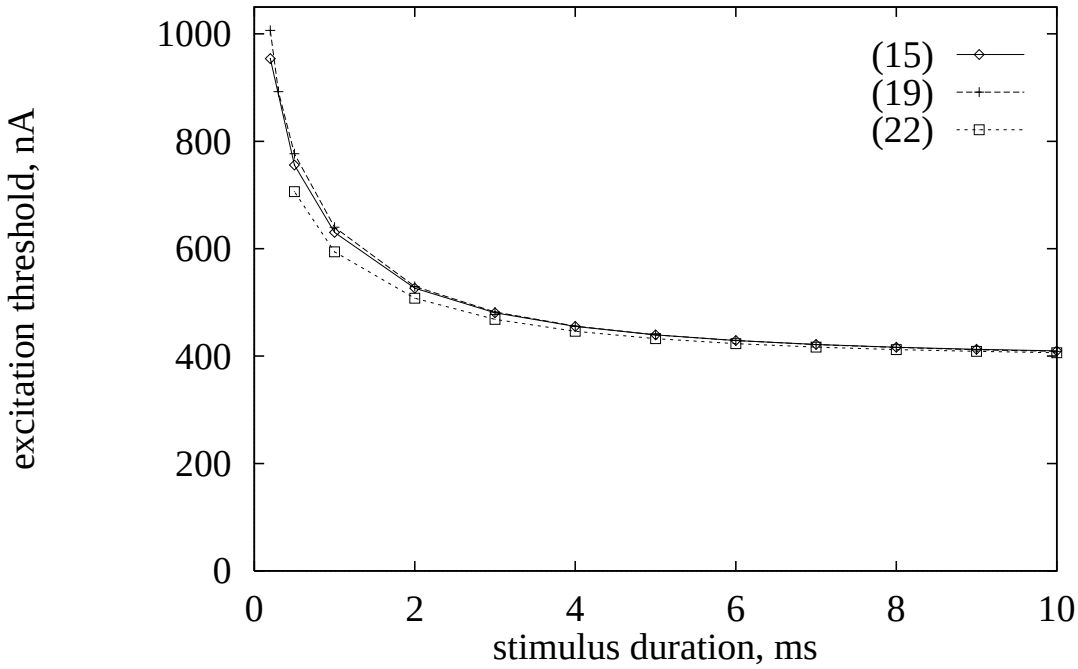

Figure 1: Strength-duration curve for a single isolated cell excited by an extracellular current pulse. $\diamond$: computed with two-point evaluation of integral, model (15). $+$: quasi-stationary model (19), $\square$: computed with five-point evaluation of integral, model (22).

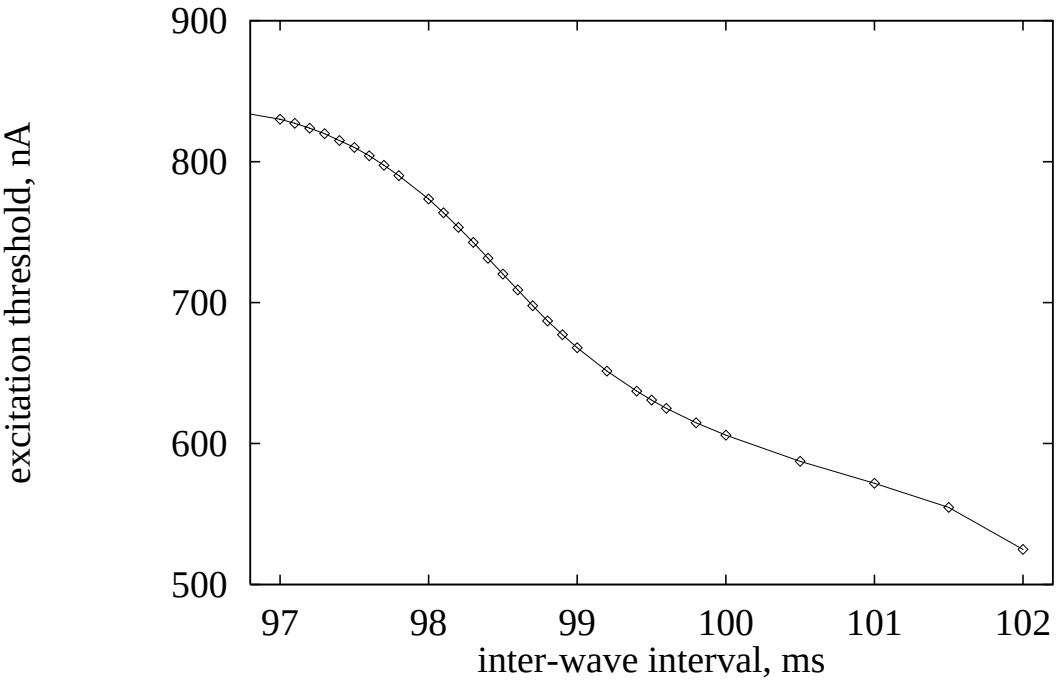

Figure 2: Excitation threshold of a single cell excited by an extracellular current pulse of 2 ms duration computed using model (19), as a function of time since the beginning of the last conditioning action potential, in model (19). To ensure that the state variables were close to those found during re-entry, the cell was conditioned by a train of action potentials obtained from a re-entrant spiral solution; the inter-wave interval is the interval between the minimum of u of the previous excitable gap, to the start of the current pulse.

7 Action onto an Excitable Fibre

The generalization of equations (19) for spatially extended tissue is straightforward as the deviation of each individual cell from an isopotential state takes place only during the short time periods of external stimulation, and outside these periods cable theory gives

$$\begin{aligned} \partial_t U &= \frac{1}{2C}(f(U+\frac{1}{2\alpha}I_{ext}(t),v_+,W)+f(U-\frac{1}{2\alpha}I_{ext}(t),v_-,W))+D\partial_x^2 U \\ \partial_t v_\pm &= g(U\pm\frac{1}{2\alpha}I_{ext}(t),v_\pm,W) \\ \partial_t W &= h(U,\frac{v_++v_-}{2},W), \end{aligned} \tag{23}$$

where U, $v_\pm$ and V are now functions not only of time t, but also of distance along the fibre x, and the diffusion coefficient for voltage, D, is proportional to the intercellular conductivity. $D = 31.25$ mm^2/s gives a conduction velocity of about 350 mm/s for a solitary wave through resting tissue. The value of D is necessary only for the interpretation of spatial scales as equations (23) are invariant under simultaneous change of spatial scales and coefficient D.

8 On the Asymptotic Theory of Defibrillation

We now apply this approach to evaluate the defibrillation threshold for a tissue, *i.e.* the amplitude of an externally applied current pulse necessary to abolish all propagating waves, and compare it with the prediction of the asymptotic theory of defibrillation for our model. The theory was described by Pumir & Krinsky [1996] and is based on separate consideration of the slow and fast processes during the process of propagation [Fife, 1976, Tyson & Keener, 1988]. During re-entrant activity and fibrillation, propagation in the whole heart is an irregular and changing pattern of waves and wavelets [Gray & Jalife, 1996]. The asymptotic theory of defibrillation assumes that on the fast time scale the medium has two alternative stable equilibria, which depend on the slow variables. The propagation of the wavefront, in the fast time scale, is a trigger wave between the equilibria that is either "antegrade", when the excited region grows, or "retrograde" propagation, when the excited region shrinks. The wavefront of a propagating pulse is an antegrade trigger wave, and its back a retrograde wave. In a resting medium, the upper, "excited" equilibrium is more stable, so a suprathreshold perturbation produces an antegrade trigger wave, and the excited region expands. During the excited state, the evolution of the slow variables lowers the stability of the excited state while the stability of the resting state increases, until a retrograde trigger wave can propagate.

In this approximation a wavefront cannot spontaneously change direction of propagation. When a defibrillating shock is applied to the whole medium, if the intensity of the shock is high enough, then all the cells of the medium can be thrown into the excited state, and thereafter only retrograde waves will occur throughout the medium and these will trigger all the medium into the resting state. Driving all the medium into the excited state provides a simple understanding of defibrillation. However it is not necessarily exact. First, not all the cells may be excitable, *i.e.* have the alternative "upper equilibrium" at the moment of shock delivery. Second, the requirement of all the excitable cells to be triggered into the excited state is excessive. Defibrillation requires that only retrograde waves are generated after it. To ensure this, it is only necessary to excite all those cells which have the resting state as the more stable state, and it is not necessary to excite those which have the excited state as the more stable.

The boundary between these classes of cells is in the state space of the slow variables, and corresponds to the values of these variables when the two equilibria are equally stable. If u is much faster than both v and w, this "equal stability" is represented by a "Maxwell rule", for the right-hand side of the fast excitability equation:

$$\int_{u_{resting}(v,w)}^{u_{excited}(v,w)} f(u,v,w)du = 0. \tag{24}$$

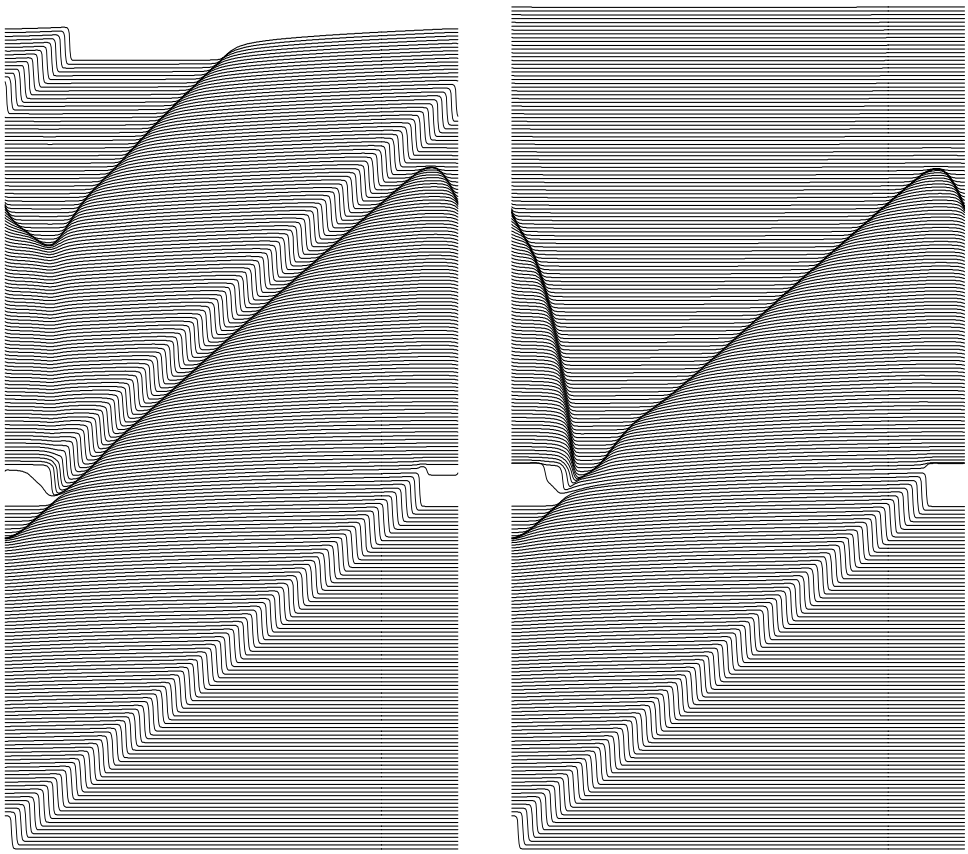

Figure 3: (a) Subthreshold (600 nA, 2 ms) and (b) suprathreshold (800 nA, 2 ms) response of a re-entrant wave in one-dimensional ring to a defibrillating shock. In both cases the wavefront is initially advanced, in the suprathreshold case the wavefront collapses back to its position at the time the pulse was applied, and meets its waveback. The circumference of the ring is 60 mm, and the membrane potential is displayed every 2 ms, *i.e.* the conduction velocity of the wave before defibrillation was 300 mm/s.

When there is only one slow variable w, as in the FitzHugh-Nagumo system considered by Pumir & Krinsky [1996], this equality has a unique solution at the "critical value" w_{cr}, and the defibrillation condition is then reduced to the requirement, that all cells with $w < w_{cr}$ should be excited. However,the "Maxwell point" falls exactly at the centre of symmetry of the excitability model used by Pumir & Krinsky [1996], $f(u, v, w) = F(u) - w$ with a cubic F, and for this model, in the style of (14), a cell at the critical point cannot be excited by a uniform field of any magnitude.

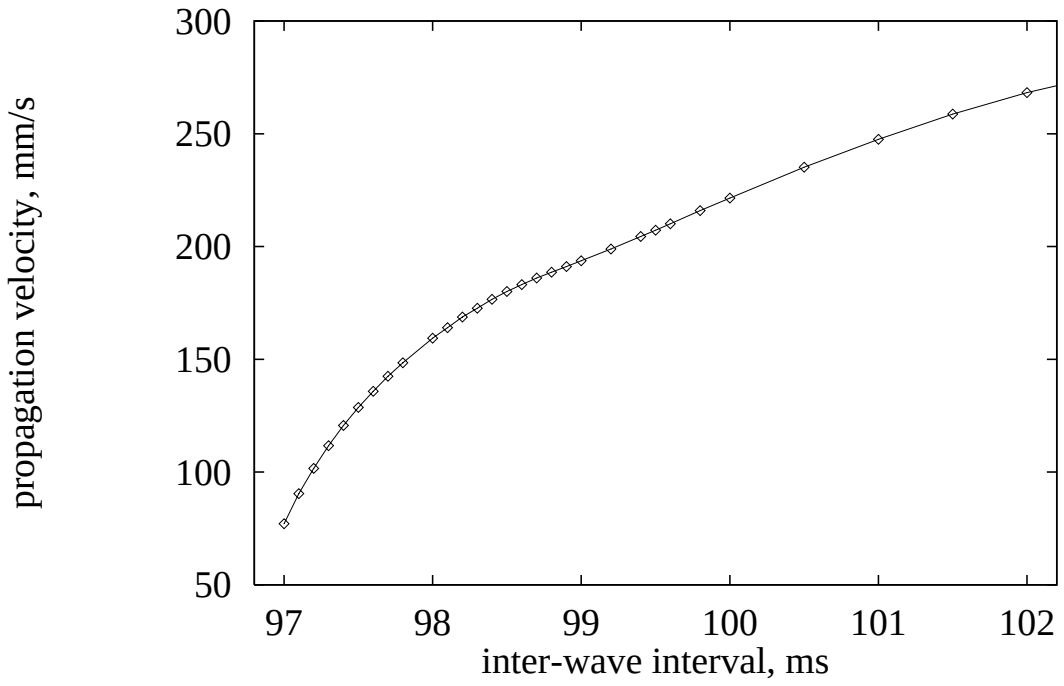

Figure 4: Velocities of forward fronts of excitation waves, mm/s, as functions of interwave intervals, ms.

In biophysical excitation equations there is no such symmetry and so the theory is applicable as long as the realistic "slow processes" v and w are slow enough for the asymptotic approach to be valid. The margin (24) between preferably-excited and preferably-resting cells is a manifold of codimension 1, and so finding the exact defibrillation condition would imply finding the points with the highest threshold on this manifold. We do not need to search the whole space, only in a subset, corresponding to states of cells present in the tissue in the moment of defibrillation. Estimation of the defibrillation threshold requires a model of fibrillation, as well as a model for the defibrillation process. We estimated the velocities of propagation of wavefronts of excitation pulses driven at the highest possible frequencies, provided by a spiral wave solution. Since, as it was mentioned in Section 7, the excitation properties are strongly influenced by the pre-history of excitations, we used here exactly the same pre-conditioning procedure as for Fig. 2. The dependence of premature pulse propagation velocity on the coupling interval is shown in Fig. 4. A 1.5 mm long one-dimensional model governed by (23) without external current was integrated with boundary conditions $u(x_0, t) = U(t)$ at one end, and non-flux condition on the other, where $U(t)$ was the transmembrane voltage profile of a developing spiral wave solution recorded at a point far from the core (see Fig. 2(b) in [Biktashev & Holden 1996], point 'D'). Thus, pulses propagated through the fibre in the same sequence as they typically do in 2D during development of a spiral wave. After

14 such pulses, the 15th one was initiated prematurely with a controlled advance in time, and its velocity was measured via crossing times at points distant 0.5 and 1.0 mm from the boundary. The smallest coupling interval we could obtain was 97 ms. Comparison with the threshold-interval plot (Fig. 2), gives the excitation threshold corresponding to this interval of 840 nA, and this provides the estimate of the defibrillation threshold. This theoretical estimate has been obtained from the threshold-interval relation for the ODE models including the models of external action (15), (19) and (22), and from the velocity-period relation for one-dimensional experiments without any external action, connected by the asymptotic theory of defibrillation. An independent "direct" estimation of this threshold was made in experiments with model (23), which is both spatially extended and involves external stimulation. For a one-dimensional fibre with periodic boundary conditions a uniform external field can extinguish a recirculating wave; the stimulus pulse forces the wavefront forward, and the wavefront then decays back to its position at the time of stimulation, while waveback continues to propagate (Fig. 3). All activity is extinguished when the waveback meets the wavefront. The resulting defibrillation threshold for these computations is 740 nA, which is similar to the "theoretical" estimation of 840 nA.

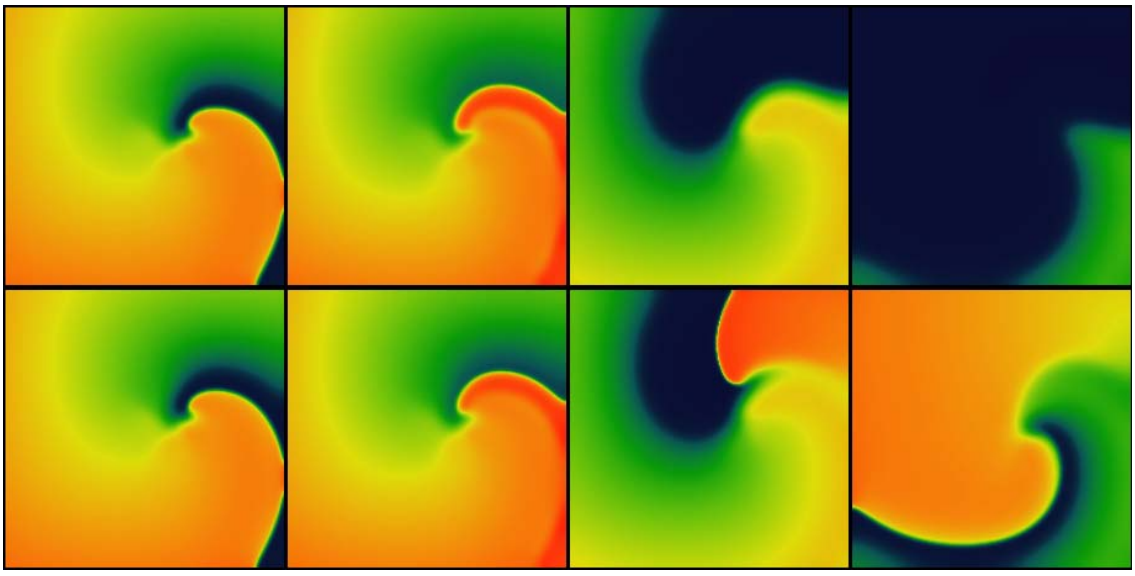

Figure 5: Snapshots from movies of suprathreshold (above, with 800 nA/cell) and subthreshold (below, with 650 nA/cell) defibrillation by a spatially uniform 2 ms depolarising current pulse of a spiral wave in a model of a 20×20 mm slice of ventricular tisue, with $\delta t = 0.05$ ms and $\delta x = 0.1$ mm, and cellular excitability described by the Oxsoft guinea pig ventricular model [Noble 1990, Biktashev & Holden 1996].

For a spiral wave solution of the two-dimensional analogue of (23), there is a narrow gap between between waveback of the spiral wave and the following wavefront. The response of such a counter-clockwise rotating re-entrant spiral (Fig. 5, 6) to a brief defibrillating pulse is similar to that seen in the one-dimensional model: the wavefront is forced forward, and then relaxes back to its position at the time the shock was applied, while the waveback continues to rotate counter-clockwise. All activity is extinguished when the waveback reaches the wavefront. The effect of the defibrillating pulse is mainly determined by the behaviour of the wavefront just after its application: if it was strong enough to make the front jump ahead into a region of refractory medium where it cannot propagate but instead retracts, then it continues to retract and so the defibrillation is successful as all activity is extinguished. The predominance of the effect on the wavefront follows naturally from the fact that the wavefront is determined by the fast processes, with a time constant τ_f close to the duration of the defibrillating shock. In this particular model, the defibrillation threshold was found to be 750 nA.

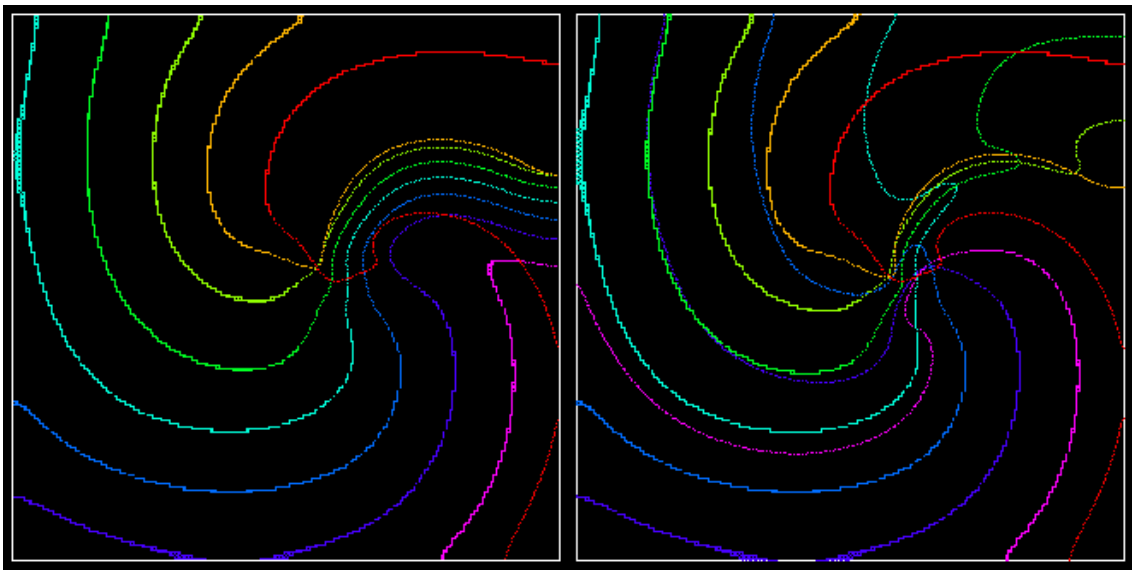

Figure 6: Wavefronts and wavebacks visualised as -10mV isolines every 10 ms during (left) the suprathreshold and (right) subthreshold defibrillating shocks of Fig. 5. The red isoline is just before the defibrillating pulse was applied; the spiral wave is rotating counterclockwise.

Since the external currents occurring in our calculations are in nA per cell, we cannot directly compare these results with clinical or experimental data. However, the dimensionless ratio between the excitation and defibrillation thresholds can be compared. In our model, this ratio has been found to be about 1.5.

Real cardiac tissue is heterogeneous and so the experimental estimation of the excitation threshold gives the threshold for the most excitable tissue, while the experimental estimation of the defibrillation threshold gives the threshold for elimination of the activity in all the tissue. Thus the exprimental ratio will always be more than this theoretical value, — *e.g.* , the ratio mentioned by Dillon [1991] is about 10.

9 Discussion

In spite of its practical importance, the processes of defibrillation still remain obscure. Most theoretical approaches have been based on linear models [Knisley *et al.* , 1994; Sepulveda *et al.* , 1989; Krassowska *et al.* , 1990], while some numerics of nonlinear models [Cartee, 1992] and theoretical studies with simplified models have been attempted [Pumir & Krinsky, 1996]. The reason for this lack of progress is the combination of nonlinearity and the hierarchical multi-timescale structure of biophysical excitation equation with the necessity for a representation of the complicated spatial structure for every cell. We have overcome these problems by applying a series of well known methods, to fullfill nonlinear averaging; the result is the simplified models of (19) and (23). This reduction of an infinite dimensional system to an ordinary differential system may be of value in a range of applications of nonlinear science.

These simplified models have been verified numerically and allow us to use biophysically detailed excitation equations, and so we are now in a position to provide a quantitative, theoretical explanation for the effects of changes in parameters in the excitation equations on the defibrillation threshold, and to design optimal defibrillation pulse parameters. Experimental techniques now exist [Zhou *et al.* , 1995] for testing such quantitative descriptions of the mechanisms of defibrillation.

Acknowledgement:

This work is supported by the Wellcome Trust(042352, 044365), the EPSRC ANM initiative (GR/J35641) and GR/K 49775. We are grateful to A. Pumir and V. Krinsky for encouraging discussions.

References

[1] Biktashev, V.N. & Holden, A.V. [1996] "Re-entrant activity and its control by resonant drift in a two-dimensional model of isotropic homogeneous ventricular tissue", *Proc. Roy. Soc. Lond.* **B 263**, 1373–1382.

[2] Boyett, M.R., Clough, A., Dekanski, J. & Holden, A.V. [1996] "Modelling cardiac excitation and excitability", in *The computational biology of the heart*, eds. Panfilov, A.V. & Holden, A.V. (J.Wiley, Chichester).

[3] Cartee, L.A. & Plonsey, R. [1992] "Active response of a one-dimensional cardiac model with gap junctions to extracellular stimulation ", *Medical and Biological Engineering and Computing* **30**, 389–398.

[4] Dillon, S.M. [1991] "Optical recordings in rabbit heart show that defibrillation strength shocks prolong the duration of depolarization and the refractory period", *Circulation Research* **69**(3), 842–856.

[5] Gray, R.A. & Jalife, J. [1996] "Spiral waves and the heart", *Int. J. Bifurcation and Chaos* **6**(3), 415–435.

[6] Fife, P.C. [1976] "Boundary and interior transition layer phenomena for pairs of second-order differential equations, *J. Math. Anal. Appl.* **54**, 497-521.

[7] Keener, J.P. [1996] "Direct activation and defibrillation of cardiac tissue" *J. Theor. Biol.* **178**, 313–324.

[8] Knisley, S.B., Hill, B. & Ideker, R.E. [1994] "Virtual electrode effects in myocardial fibres" *Biophys. J.* **66**, 719–728.

[9] Krassowska, W., Frazier, D.W., Pilkington, T.C. & Ideker, R.E. [1990] "Potential distribution in three-dimensional anisotropic medium", *IEEE Biomed Eng* **37**, 267–284.

[10] Krassowska, W. & Neu, J.C. [1994] "Response of a single cell to an external electric field", *Biophys. J.* **66** 1768–1776.

[11] Noble, D. [1990] Oxsoft HEART version 3.8 manual (Oxsoft, Oxford)

[12] Panfilov, A.V. & Holden, A.V. (eds) [1996] *The computational biology of the heart* (J.Wiley, Chichester).

[13] Plonsey, R. & Barr, R.C. [1986] "Effect of microscopic and macroscopic discontinuities on the response of cardiac tissue to defibrillating (stimulating) currents", *Medical and Biological Engineering and Computing* **24**(2), 130–136.

[14] Pumir, A. & Krinsky, V. [1996] "How does an electric current defibrillate cardiac muscle" *Physica D*, **91**, 205–219.

[15] Tyson, J.J. & Keener, J.P. [1988] "Singular perturbation theory of traveling waves in excitable media (a review)", *Physica D* **32**, 327-361.

[16] Sepulveda, N.G., Roth, B.J. & Wikswo, J.P. Jr [1989] "Current injection into a two-dimensional anisotropic medium" *Biophys. J.* **55**, 987–999.

[17] Weidmann, S. [1952] "Electrical constants of trabecular muscle in mammamlian heart" *J. Physiol. Lond.* **118**, 348–360.

[18] Zhou, X., Ideker, R.E., Blitchington, T.F., Smith, W.M. & Knisley, S.B. [1995] "Optical transmembrane potential measurements during defibrillation-strength shocks in perfused rabbit hearts", *Circulation Research* **77**, 593–602.

[19] Zipes, D.P. & Jalife, J. (eds) [1995] *Cardiac Electrophysiology - from Cell to Bedside* (W.B.Saunders, Philadelphia).